*Materials Science-Poland*, *Vol. 26*, *No. 3*, *2008*

# New magnetic Ni-Al hydrotalcite-like materials Synthesis and characterization

J. WANG*, J. YOU, P. YANG, C. ZHONG, Z. LI, M. ZHANG, X. JING

School of Material Science and Chemical Engineering, Key Laboratory of Science and Technology of Controllable Chemical Reactions, Harbin Engineering University, Harbin 150001, PR China

Novel magnetic Ni-Al hydrotalcite with Ni/Al molar ratio of 3 was synthesized by the hydrothermal method and co-precipitation. The obtained material was characterized in detail by thermogravimetric analysis – differential scanning calorimetry, X-ray diffraction (XRD), transmission electron microscopy (TEM), and vibrating sample magnetometry (VSM). XRD analysis indicated that a more well-crystallized hydrotalcite-like phase and higher thermal stability were present in the hydrothermally treated product than in that obtained by the conventional co-precipitation method. Well-defined flat particles were observed by TEM, and the (200) lattice plane ($d$ = 0.21 nm) could be clearly seen in the HRTEM image. Furthermore, VSM results showed that the obtained material exhibited paramagnetism.

Key words: *hydrotalcite; magnetism; hydrothermal method; co-precipitation*

## 1. Introduction

Hydrotalcites (HTLcs) are commercially available and cheap solid bases; hydrotalcites and calcined hydrotalcites (normally referred to as mixed oxides) are highly active, selective catalysts and play an important role in many base-catalyzed reactions, such as Claisen–Schmidt condensations [1] and Knoevenagel condensations [2]. However, the problems of separation, recovery and pollution limit their industrial applications. The separation methods for these solid mixed oxides need extra equipment and treatments, which consume a great deal of energy and money. Therefore, it is essential to synthesize a novel solid base catalyst to extend the utility of catalysts and develop green routes. The drive to develop environmentally benign processes has led to a considerable increase in research activities both in academic and industrial sectors for the development of solid base catalysts. Based on the above consideration, Carja et al. [3] reported new magnetic layered structures which can be used as precursors for new

*Corresponding author, e-mail: zhqw1888@sohu.com

hybrid nanostructures such as aspirin-hydrotalcite-like anionic clays. Srikanth et al. [4] reported the synthesis of super-paramagnetic $Fe_3O_4$ nanoparticles recently. The presented $Fe_3O_4$ possesses uniform crystallite size (about 11 nm) and high-dispersion.

Co-precipitation is the most common method to synthesize HTLcs which is based on the reaction of a solution containing $M^{II}$ and $M^{III}$ metal cations in adequate proportions with an alkaline solution. However, the crystallinity of the obtained samples is strongly affected by the synthetic parameters such as the pH value, temperature, concentration of used solutions and others [5–7]. Hydrothermal synthesis is a well-known and established method to prepare transition metal oxides and other well-crystallized samples [8–10]. It is well-known that the catalytic performance of hydrotalcite is dramatically increased through the incorporation Ni into the hydrotalcite material. The formation of surface-enriched Ni in the hydrotalcite seems to be the main reason for its high catalytic performance [11].

In our present work, two methods have been used to obtain the magnetic Ni-Al hydrotalcites: one method is based on the direct co-precipitation synthesis by using $Fe_3O_4$ as magnetic core, the other one is based on the hydrothermal treatment by the introduction of $Fe_3O_4$ endowed Ni-Al HTLcs with magnetism which makes it possible to achieve the ease of recovery and recycling of HTLcs through an external rotating magnetic field. New results are reported for the first time, to the best of our knowledge. This novel magnetic Ni-Al HTLcs is expected to be used as a green catalyst, and thus solve the disadvantages as mentioned above.

## 2. Experimental

*Synthesis*. Magnetic nanoparticles were prepared by dissolving 0.01 mol of $FeSO_4$ and 0.01 mol of $Fe_2(SO_4)_3$ in water, under stirring at 45 ºC, and 20 wt. % of $NH_3{\cdot}H_2O$ were added dropwise together at a constant pH value of 10–11. The obtained material ($Fe_3O_4$) was recovered, washed several times with de-ionized water until the pH was neutral. The obtained $Fe_3O_4$ was preserved as a suspension.

An aqueous solution containing 17.45 g of $Ni(NO_3)_2{\cdot}6H_2O$ and 7.5 g of $Al(NO_3)_3{\cdot}9H_2O$ was added dropwise to $Fe_3O_4$ solution with Ni/Fe molar ratio equal to 50 under vigorous stirring. During the synthesis, the temperature was maintained at 60 °C and pH at about 11 by simultaneous addition of NaOH and $Na_2CO_3$ solution. The resulting mixture was transferred to an autoclave pressure vessel and hydrothermally treated at 200 °C for 10 h. When the autoclave temperature reached the room temperature, the product was removed, filtered, washed with distilled water to get netural pH, and dried at 80 °C for 24 h. The resulting sample was calcined at various temperatures between 200 °C and 900 °C for 5 h.

Magnetic Ni-Al HTLcs was also prepared by the direct co-precipitation method, in order to compare with the obtained hydrothermally treated sample. An aqueous solution containing $Ni(NO_3)_2{\cdot}6H_2O$ and $Al(NO_3)_3{\cdot}9H_2O$ was added dropwise to the above synthesized $Fe_3O_4$ solution with Co/Fe molar ratio equal to 50 under vigorous stirring.

During the whole synthesis, the temperature was maintained at 65 °C and the pH at about 10 by the simultaneous addition of NaOH and $Na_2CO_3$ solution. When enough reaction time had elapsed, the product was removed, filtered, washed with distilled water to get neutral pH, and dried at 80 °C for 24 h.

*Characterization*. Thermogravimetric analysis – differential scanning calorimetry (TG-DSC) of the as-synthesized sample was performed on a NEZSCH STA 409PC thermoanalyzer. The analysis was carried out in Ar atmosphere in the temperature range 40–600 °C with the heating rate of 10 °C/min. Powder X-ray diffraction (XRD) patterns were recorded on a Rigaku D/max-IIIB diffractometer using $CuK_\alpha$ radiation ($\lambda = 0.15406$ nm). Transmission electron microscopy (TEM) and high-resolution transmission electron microscopy (HRTEM) experiments were performed using a Philips CM 200 FEG electron microscope with an acceleration voltage of 200 kV. The samples were dispersed in ethanol. Carbon-coated copper grids were used as the sample holders. Magnetic hysteresis loops were measured using a vibrating sample magnetometer (VSM, JDAW-2000). For magnetization measurements, the powder was pressed strongly and fixed in a small cylindrical plastic boxes.

## 3. Results and discussion

### 3.1. TG-DSC studies

The TG-DSC curves of the magnetic Ni-Al HTLcs treated by hydrothermal method and co-precipitation method are shown in Fig. 1. Both the TG-DSC profiles of magnetic Ni-Al HTLcs exhibited two apparent endothermic events, and two distinc-

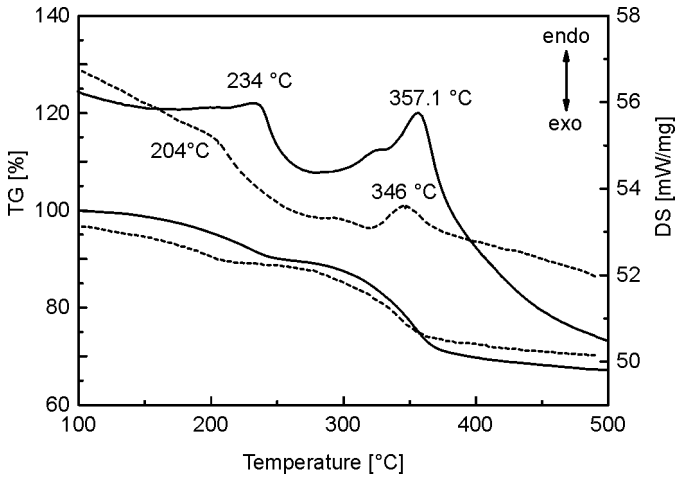


Fig. 1. TG-DSC curves of magnetic Ni-Al HTLcs synthesized by hydrothermal treatment (solid lines) and conventional co-precipitation (dashed lines)

tive steps of weight loss. The DSC profile of hydrothermally treated samples (solid lines) exhibited two apparent endothermic peaks at 234 and 357.1 °C, with a minor, broad endothermic peak at about 324 °C. This also can be proved by the TG curve, where two clear weight losses can be observed. At the first stage, the weight loss can be assigned to the loss of physically absorbed (surface) and interlayer water [12–14], in the diagram of TG curve, 8.44 % loss was observed. Based on this value, the water content was estimated to be 2.34 per chemical formula. The second one can be assigned to the loss of hydroxyl ions and removal of carbonate ions. Notably, the TG-DSC profiles for magnetic Ni-Al HTLcs synthesized by direct co-precipitation (broken lines) showed two apparent endothermic peaks at 204.1 °C and 346 °C, which was slightly lower than hydrothermal treatment showed. This indicated that the sample possessed high thermal stability which can be further demonstrated by the following XRD and TEM observations.

### 3.2. Powder X-ray diffraction XRD

The XRD patterns of magnetic Ni-Al HTLcs synthesized by hydrothermal method (A) and co-precipitation method (B) are shown in Fig. 2. In both samples, there appeared diffraction peaks corresponding to the layered double hydroxides structure. In concrete, the sharp symmetric reflections of the basal (003), (006) and (009) planes; broad, less intense and asymmetric reflections for the nonbasal (012), (015) and (018) planes were observed.

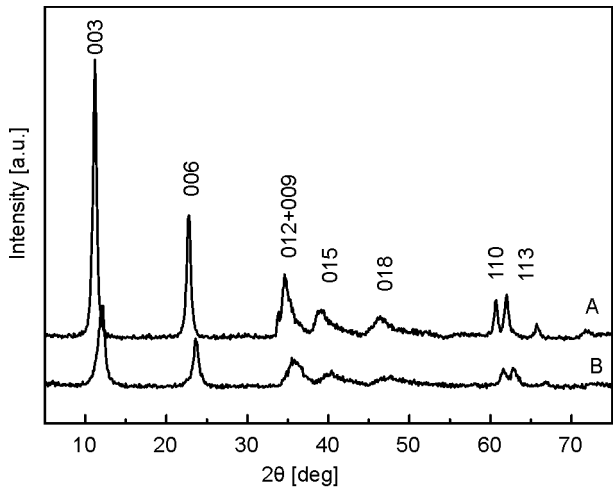


Fig. 2. XRD patterns of magnetic Ni-Al HTLcs synthesized by hydrothermal treatment (A) and conventional co-precipitation (B)

At the same time, (009) and (012) reflections partially overlapped in the $2\theta$ range of 33–37°. All of these features were characteristic of a typical hydrotalcite-like

phase [15]. No typical diffraction peak of iron oxides was observed for Fe-LDH sample, which showed that the magnetism ($Fe_3O_4$) was highly dispersed in the hydrotalcite structure. It should be noted that the hydrothermal treatment resulted in an increasing intensity of diffraction peaks. Furthermore, after the hydrothermal treatment, the typical XRD diffraction peaks shift to lower angles, which implied the increase of the interlayer spacing and growth of crystallites. The growth of crystallites can be explained: the amorphous part of the co-precipitated sample dissolves during hydrotalcite synthesis under hydrothermal conditions, which results in the increase of hydrotalcite content.

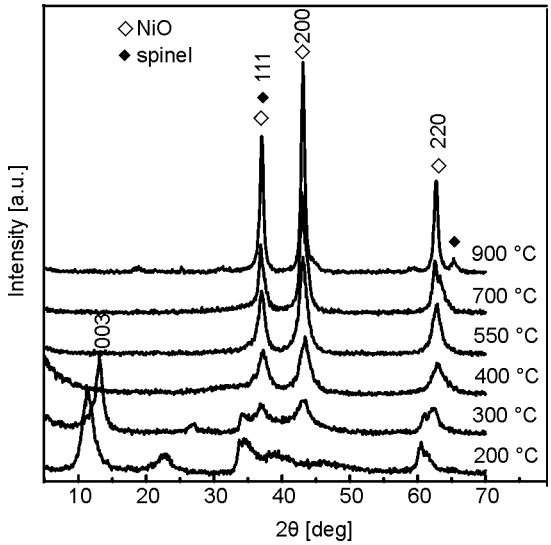


Fig. 3. XRD patterns of hydrothermally treated magnetic Ni-Al HTLcs calcined at various temperatures

In order to investigate the effect of calcination temperature on the structure of hydrothermally treated magnetic Ni-Al HTLcs, the samples calcined at various temperatures were characterized by XRD. As shown in Fig. 3, the presented XRD pattern of magnetic Ni-Al HTLcs calcined at 200 °C was similar to that of the dried sample obtained by hydrothermal treatment, which indicates the obtained calcined sample still possesses a layered double structure. However, the XRD diffraction peaks, especially for (003), of the calcined sample shifted to higher angles when the temperature was increased to 300 °C. The decomposition of the hydroxide layers and the removal of interlayer anions (carbonate) resulted in the decrease of the interlayer spacing, and thus the shift of XRD diffraction peaks which was consistent with the TG-DSC results. It should be noted that, at this temperature, the characteristic (200) peaks of NiO were evident. Further increase of the calcination temperature led to the complete decomposition of HTLcs and the formation of single oxide NiO (cubic structure, JCPDS 4-835). The (110), (200), and (200) diffraction peaks can be clearly seen in Fig. 3.

With the increase of calcination temperature, these diffraction peaks became more narrow and intense, which can be attributed to the growth of crystallites and improvement of crystallization. For the conventional Ni-Al HTLcs, $NiAl_2O_4$ was formed as a crystalline phase at 800 °C. However, for our obtained sample, even if the temperature was increased to 900 °C, the calcined sample can also possess the single NiO crystalline phase after thermal decomposition. This can be ascribed to the hydrothermal treatment and the introduction of $Fe_3O_4$ during the synthetic process. The $Al^{3+}$ ions can either be incorporated in an amorphous nickel aluminate phase, or in a separate amorphous alumina phase [16]. Single NiO crystalline phase maintained at high temperature is particularly important for applications in catalysis and electrochemistry fields. Moreover, it exhibited spinel phase ($Ni_aFe_bAl_cO_d$) when the calcination temperature increased to 900 °C. Mixed oxides involving spinel as a basic catalyst can be used in multiform catalytic reactions.

### 3.3. Transmission electron microscopy (TEM)

The morphology of a hydrothermally treated magnetic Ni-Al HTLcs sample without calcination was investigated by TEM. The TEM images are shown in Fig. 4. The flat particle morphology was observed to be regular, and of hexagonal shape throughout. The grain boundaries were well defined and the platelet size was about 200 nm. A dissolution and re-crystallization of the smallest crystallites and amorphous parts during hydrothermal treatment should be responsible for the large particle size.

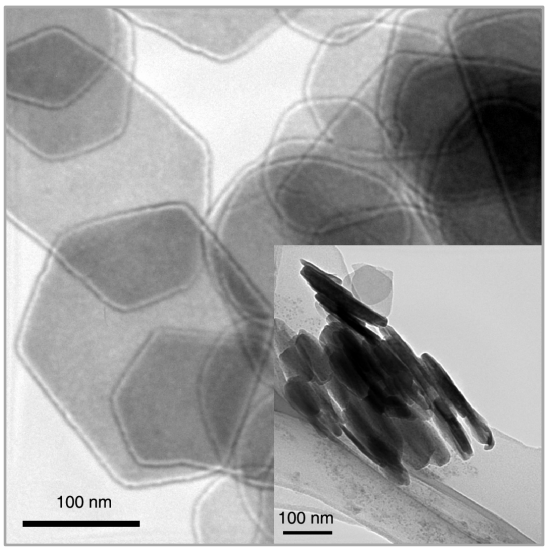


Fig. 4. TEM image of magnetic Ni-Al HTLcs without calcination

The increase in both crystallinity and crystallite size upon hydrothermal treatment was further confirmed by the XRD observations. No diffraction fringes were observed, although the sample was crystalline, as evidenced by the XRD pattern. However, it should be remembered that in the experimental conditions, necessary for TEM analysis, the samples were kept under high vacuum. Therefore, it seemed reasonable to assume that a deep dehydration and a partial loss of the layered structure occurred. The inset of Fig. 4 shows the profile of the sample. It can be clearly seen that the thin plates composed of layered structures and the thickness of the platelet was about 17 nm.

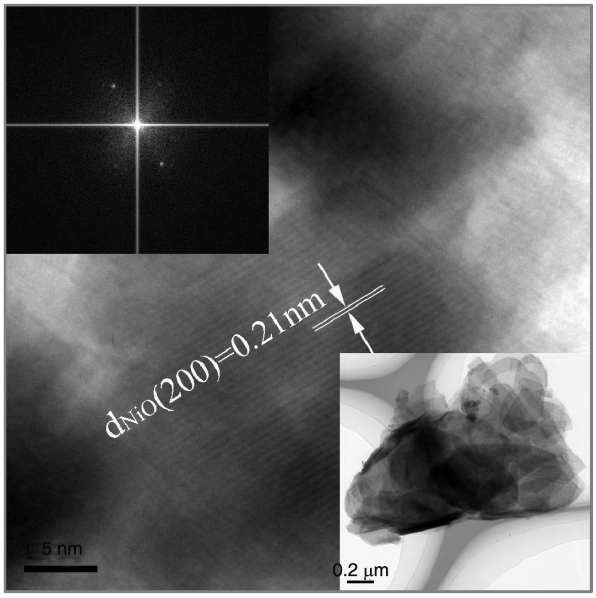


Fig. 5. TEM image and the corresponding Fourier diffractogram (inset) of magnetic Ni-Al HTLcs calcined at 300 °C

Figure 5 shows typical TEM images at various magnifications of hydrothermally treated magnetic Ni-Al HTLcs calcined at 300 °C. The micrograph at lower magnification (the inset of Fig. 5) clearly shows the structure of HTLcs that had been partly destroyed by calcination. The lattice fringes can be easily observed from the HRTEM image. The lattice fringe corresponding to (200) ($d$ = 0.21 nm) crystallographic planes of NiO was presented in Fig. 5, which was consistent with the Fourier diffractograms shown in the inset of Fig. 5. The TEM observations were in good agreement with XRD results.

### 3.4. Vibrating sample magnetometry (VSM)

Figure 6 shows the hysteresis curves of hydrothermally treated magnetic Ni-Al HTLcs without calcination. The Ni/Fe molar ratio was 50. The magnetic properties,

such as saturation magnetization ($M_s$), remanent magnetization ($M_r$) and coercivity ($H_c$), are given in Table 1. The hysteresis curve of the hydrothermally treated magnetic Ni-Al HTLcs exhibited a paramagnetic behaviour ($M_s$ = 2.09 emu/g and $H_c$ = 0 Oe). It demonstrated that the obtained sample exhibited paramagnetism which can be attributed to the $Fe_3O_4$ particle with very small particle size [4]. However, the specific saturation magnetization decreased to 1.88 emu/g when the ($FeO_x$/Fe-HTLcs)

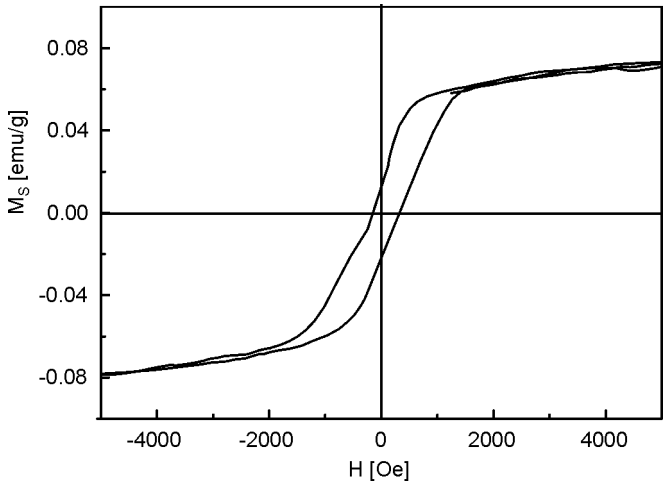


Fig. 6. Magnetic hyteresis curve of magnetic Ni-Al HTLcs without calcination

sample was calcined at 400 °C, which can be due to the change of magnetic valence. XRD pattern of the sample calcined at 400 °C showed metal oxide (NiO) formation, as shown in Fig. 3. Non-magnetic substances, such as NiO, may impede the magnetization orientation of the product and result in the decrease of the magnetism. From Table 1, it can be observed that the coercivity ($H_c$) of the sample calcined at 400 °C was 339 Oe. The increase in the $H_c$ value was attributed to adhesion and growth of the crystal grains, which resulted in a change from paramagnetism to ferrous magnetism in the Ni-Al HTLcs.

Table 1. The magnetic capability of magnetic Ni-Al HTLcs
(Ni/Fe molar ratio equal to 50)

| | Calcination temperature [°C] | |
|---|---|---|
| | 0 | 400 |
| $M_s$ (emu/g) | 2.09 | 1.88 |
| $M_r$ (emu/g) | 0.37 | 0.37 |
| $M_r/M_s$ | 0.178 | 0.198 |
| $j_{Hc}$ [$O_e$] | 0 | 339 |

## 4. Conclusions

We introduced a simple synthesis route to prepare the magnetic Ni-Al HTLcs on the basis of the hydrothermal treatment method. The hydrothermally treated magnetic Ni-Al HTLcs presented higher thermal stabitlity in comparison with the sample in the absence of hydrothermal treatment. Furthermore, the obtained materials exhibited paramagnetism. This novel material has potential applications as a green catalyst or as a catalyst-support. We expect this novel synthetic method can be extended to the synthesis of other magnetic HTLcs.

**Acknowledgement**

We gratefully acknowledge the support of this research by the Key Technology R&D program of Heilongjiang Province (no.G202A423, no.TB06A05), and by the Science Fund for Young Scholar of Harbin City (no. 2004AFQXJ038).

## References

[1] CLIMENT M.J., CORMA A., IBORRA S., PRIMO J., J. Catal., 151 (1995), 60.
[2] CORMA A., FORNÉS V., MARTIN-ARANDA R.M., REY F., J. Catal., 134 (1992), 58.
[3] CARJA G., CHIRIAC H., LUPU N., Magn J., Magn. Mater., 311 (2007), 26.
[4] GASS J., PODDAR P., ALMAND J., SRINATH S., SRIKANTH H., Adv. Funct. Mater., 16 (2006), 71.
[5] KOVANDA F., KOLOUŠEK D., CÍLOVÁ Z., HULÍNSKÝ V., Appl. Clay Sci., 28 (2005), 101.
[6] CARPENTIER J., LAMONIER J.F., SIFFERT S., ZHILINSKAYA E.A., ABOUKAÏS A., Appl. Catal. A, 234 (2002), 91.
[7] KUŚTROWSKI P., SULKOWSKA D., CHMIELARZ L., RAFALSKA-LASOCHA A., DUDEK B., DZIEMBAJ R., Microporous Mesoporous Mater., 78 (2005), 11.
[8] LABAJOS F.M., RIVES V., ULIBARRI M.A., J. Mater. Sci., 27 (1992), 1546.
[9] RAO M.M., REDDY B.R., JAYALAKSHMI M., JAYA V.S., SRIDHAR B., Mater. Res. Bull., 40 (2005), 347.
[10] KOOLI F., KOSUGE K., TSUNASHIMA A., J. Solid State Chem., 118 (1995), 285.
[11] JANA S.K., WU P., TATSUMI T., J. Catal., 240 (2006), 268.
[12] YUN S.K., PINNAVAIA T.J., Inorg. Chem., 35 (1996), 6853.
[13] KLOPROGGE J.T., HICKEY L., FROST R.L., J. Solid State Chem., 177 (2004), 4047.
[14] TAKEHIRA K., KAWABATA T., SHISHIDO S., MURAKAMI K., OHI T., SHORO D., HONDA M., TAKAKI K., J. Catal., 231 (2005), 92.
[15] XU Z.P., XU R., ZENG H.C., Nano. Lett., 1 (2001), 703.
[16] PÉREZ-RAMÍREZ J., MUL G., MOULIJN J.A., Vib. Spectr., 27 (2001), 75.

*Received 8 July 2007*
*Revised 4 June 2008*